International Journal of Modern Physics A

PHYSICAL CONDITIONS IN NEARBY ACTIVE GALAXIES CORRELATED WITH ULTRA-HIGH-ENERGY COSMIC RAYS DETECTED BY THE PIERRE AUGER OBSERVATORY

SERGEY GUREEV

M.V. Lomonosov Moscow State University,
Moscow 119992, Russia

SERGEY TROITSKY

Institute for Nuclear Research of the Russian Academy of Sciences,
60th October Anniversary Prospect 7a, 117312, Moscow, Russia
st@ms2.inr.ac.ru

We analyze the active-galaxy correlation reported in 2007 by the Pierre Auger Collaboration. The signal diminishes if the correlation-function approach (counting all "source–event" pairs and not only "nearest neighbours") is used, suggesting that the correlation may reveal individual sources and not their population. We analyze available data on physical conditions in these individual correlated sources and conclude that acceleration of protons to the observed energies is hardly possible in any of these galaxies, while heavier nuclei would be deflected by the Galactic magnetic field thus spoiling the correlation. Our results question the Auger interpretation of the reported anisotropy signal but do not contradict to its explanation with intermediate-mass nuclei accelerated in Cen A.

Keywords: Ultra-high-energy cosmic rays; active galaxies; supermassive black holes

PACS numbers: 98.70.Sa

1. Introduction

Astronomy of ultra-high-energy (UHE; energy $E \gtrsim 10^{19}$ eV) cosmic rays (CRs) is a new branch of science whose birth we are currently witnessing. To identify UHECR sources is therefore an important and challenging task. Observational evidence in favour of particular sources is limited by low statistics, by systematic uncertainties in determination of the primary-particle type and energy, by deflection of charged particles in unknown cosmic magnetic fields and by other confusing effects in the analysis. Theoretically, several compelling mechanisms of UHECR acceleration have been developed and a number of potential astrophysical sources have been suggested (see e.g. Refs. [1,2] for reviews and summary). Physical conditions in potential sources are often uncertain thus preventing one from firm identification of theoretically most favoured candidates.

Recently, considerable interest has been attracted by a claim of correlation of positions of nearby active galaxies with arrival directions of UHECR particles detected by the Pierre Auger Observatory (PAO) [3,4]. The correlation was interpreted as an evidence that UHECR particles are protons either from nearby active galactic nuclei (AGN) or from other sources with a similar distribution in space. The AGN interpretation was considered likely based on the previous works favouring AGN as possible UHECR accelerators. Notably, Ref. [4] cites Ref. [5] in this context; the latter reference however studies the most powerful AGN (BL Lac type objects and optically violent variable quasars), while the analysis of Ref. [3] is based on the nearby objects listed in the Véron-Cetti& Véron catalog [6] which are mostly low-power Seyfert galaxies. In Ref. [7], we analyzed general constraints from geometry of the source and from radiation losses which restrict potential astrophysical accelerators and compared them to the most recent astrophysical data. Our study suggested that only the most powerful AGN are able to accelerate UHE particles while Seyfert galaxies *generically* are not. In this work, we apply the general constraints discussed in Ref. [7] to *particular* active galaxies correlated with Auger events.

The rest of the paper is organised as follows. In Sec. 2, we briefly review the Auger result emphasising particular details of the analysis of Refs. [3,4] and demonstrate that the correlation signal is strong only if a single nearest-neighbour potential source is counted for each event and diminishes in the correlation-function approach when every pair "event–source" is counted both in the data and in the simulations. We then select these nearest-neighbour source candidates (mostly Seyfert galaxies) for the Auger events and study, in Sec. 3, their properties. We conclude that it is unlikely that these objects can accelerate protons up to the observed energies and discuss implications of this conclusion in Sec. 4.

2. Summary and discussion of the Auger correlations

2.1. *Anisotropy reported by PAO*[a]

Recently, the Pierre Auger Collaboration reported a significant deviation from isotropy of the arrival directions of the highest-energy cosmic rays observed by their surface detector [3]. They studied an (unpublished) set of events with energies $E \geq 4 \times 10^{19}$ eV and cross-correlated their arrival directions with positions of active galaxies from the Véron catalog [6]. Three cuts were tuned to maximize the signal: (1) the minimal reconstructed energy of a cosmic-ray particle, $E_{\rm min}$; (2) the maximal redshift of a galaxy, $z_{\rm max}$; (3) the maximal angular separation ψ between a galaxy and a cosmic-ray arrival direction at which they are counted as correlated. An excess of correlated event–galaxy pairs over the number expected for isotropic distribution was found; the signal was maximized for $E_{\rm min} = 5.6 \times 10^{19}$ eV, $z_{\rm max} = 0.018$ and $\psi = 3.1^\circ$.

After the signal had been verified in an independent data set with the same cuts

[a]See Note Added for discussion of the most recent results.

(the probability of chance correlation in the independent set of 12 events was found to be $P \sim 1.7 \times 10^{-3}$), details of the correlations were studied in the full data set [4]. The full set was again subject to the same scans in $E_{\rm min}$, $z_{\rm max}$ and ψ; the minimal formal probability of $P_{\rm min} \sim 5 \times 10^{-9}$ occured at $E_{\rm min} = 5.7 \times 10^{19}$ eV, $z_{\rm max} = 0.017$ and $\psi = 3.2^\circ$. The part of the data set which maximizes the correlation signal (27 events) was published [4] and may be used for analysis and further studies while the full data set remains unavailable. To estimate P from $P_{\rm min}$, one may use the so-called penalty factor (see e.g. Ref. [8]) which compensates for the artificial signal obtained by tuning the cuts or, in other words, for multiple tries (see also Ref. [9] for discussion). This penalty factor should be determined by Monte-Carlo simulations [8] which are however quite lengthy for these low $P_{\rm min}$. One may estimate it roughly by counting the number of tries: the scan in $0 \leq z_{\rm max} \leq 0.024$ in steps of 0.001 gives 25 tries, the scan in $1^\circ \leq \psi \leq 8^\circ$ in steps of 0.1° gives 71 tries and the scan in $E_{\rm min} \leq 4 \times 10^{19}$ eV with unspecified step gives effectively the number of tries equal to the number of events in the sample, that is 27. Altogether, the penalty factor is roughly $25 \times 71 \times 27 \approx 4.8 \times 10^4$ (in practice, the penalty factor should be somewhat lower because the tries are not independent) and $P_{\rm est} \sim P_{\rm min} \times 4.8 \times 10^4 \approx 2 \times 10^{-4}$.

The consistency in probabilities ($P_{\rm est} \sim P$ up to an order-of-magnitude correction which may be attributed to unpublished[b] tries with other catalogs) and in the values of the tuned cut parameters in the full data set and in the first half supports that a significant deviation from isotropy, and not an outstanding chance fluctuation, was indeed observed. The interpretation of this anisotropy is however not unique. Firstly, active galaxies may serve only as a tracer of the actual sources which could be distributed in the Universe in a similar way — indeed, most potential sources follow the distribution of galaxies which locally is not uniform due to superclusters and voids. This interpretation cannot be distinguished from the simplest hypothesis that the AGN are cosmic-ray sources based on the present-level correlation signal; both are unified in the *AGN hypothesis* of the Auger collaboration: most of the cosmic rays reaching the Earth in that energy range are protons from nearby astrophysical sources, either AGN or other objects with a similar spatial distribution [3]. This interpretation requires a large (of order a hundred [4]) number of sources.

Secondly, it has been shown [11,12,13,14] that a similar signal may be easily produced in case of just a few nearby sources but larger deflection angles (consistent with the chemical composition of the cosmic rays observed by the fluorescent detector of the same Pierre Auger Observatory [15] and by the Yakutsk experiment [16]). In particular, the origin of a significant part of cosmic-ray particles in the nearby FR I radio galaxy Cen A may explain [11] the observed signal for the angular spread $\sim 10^\circ$ typical for intermediate-mass nuclei arriving from a source with these Galactic coordinates [14]. Moreover, this kind of interpretation is actually supported by statistical

[b]Or published elsewhere, e.g. in Ref. [10].

analyses of the global distribution of the arrival directions of the cosmic rays in the maximally correlated Auger sample [11]. Qualitatively, under the AGN hypothesis, a similar number of events is expected from the directions of the Virgo and Centaurus superclusters (the latter is significantly farther but the former is observed by Auger with much lower exposure). In practice, however, no events came from Virgo while the Centaurus region dominates the correlation [11]. Alternative interpretations of the Auger signal have been considered also in Refs. [17,18,19,20,21,22,23].

Thirdly, independent experiments disagree about the presence of a similar correlation in their data. Using a dataset of a similar size, the High Resolution Fly's Eye experiment (HiRes) did not find a correlation with nearby Véron AGN either by applying the PAO prescription or performing similar scans in $E_{\min}$, $z_{\max}$ and ψ [24]. The data of the Yakutsk Extensive Air-Shower Array support the correlation [25]; the strongest signal occurs at $E_{\min}$, $z_{\max}$ and ψ close to the values prescribed by PAO though the angular resolution of the experiment and possibly the energy scale are different. We note that UHECR correlations with nearby Seyfert galaxies from catalog [26] have been discovered by Uryson in 1999 [27,28] using the AGASA and Yakutsk data for somewhat lower energies $E \gtrsim 4 \times 10^{19}$ eV. However, a similar sample of Seyfert galaxies from the Véron catalog does not correlate with the same cosmic-ray sample [2].

In this paper, we analyse the observed correlation from a completely different point of view.

2.2. *Nearest neighbour or correlation function?*

In any correlation analysis similar to that of [3], the number of observed pairs "event–source" is compared to that expected from chance coincidence. The definition of the "number of pairs" is however not unique: when an event is found within the angular distance ψ from k sources and $k > 1$, the "number of pairs" may be counted either as 1 (counting only **nearest-neighbour** source for each event) or as k (counting **every source–event pair**). Clearly, the same rules should be applied both to the data set and to the Monte-Carlo sets used to estimate the expected number. While the nearest-neighbour approach may be psychologically favoured because a single cosmic-ray particle cannot originate in several sources, it is the second approach which is widely applied in statistical studies by terms of the **correlation function** between two sets of points (events and sources)[c].

For an isotropic distribution of potential sources on the sky (when clustering of sources at the angular scale $\sim \psi$ is consistent with chance coincidence), both approaches give qualitatively similar results and both may serve to test the association between the ensemble of sources and the ensemble of cosmic rays. When sources are clustered at the angular scale $\sim \psi$ (which is the case for the AGN sample used

[c]This correlation-function approach has been used in many previous UHECR correlation studies, see e.g. Refs. [2,29,30]

by PAO), it is the correlation-function approach which should be used to study the correlation between ensembles, while the nearest-neighbour method may still be used to determine particular sources. If the correlation exists with the population of (clustered) sources, one cannot say which particular objects are responsible for individual events; the correlation is a collective effect of many sources separated from the cosmic-ray arrival directions by angles $\sim \psi$. A similar effect is expected if the sample of the sources under study is just a tracer of other sources with a similar distribution. On the other hand, if the correlation-function approach reveals no signal but the nearest-neighbour approach does reveal some, this is a strong argument that some of these nearest-neighbour sources may be related to particular events (we will see below that it is precisely what happens with the Auger correlation). This statement, to be discussed in detail elsewhere, may be easily understood by comparison of two cases: a large number of weak sources versus a small number of strong sources in the sample.

The key point of the calculation of the probability of chance correlation used in PAO papers [3,4] is the calculation of the fraction of the (exposure-weighted) sky area covered by circles with radius ψ centered on the potential sources in the catalog. This fraction, called p in Refs. [3,4], allows to estimate the probability of chance correlation in the nearest-neighbour approach simply by the binomial distribution, cf. Ref. [3]. As it is illustrated in Fig. 1, p may be calculated in two different ways: in the "nearest-neighbour" approach, the total covered area of the sky is counted independently of overlaps, while in the correlation-function approach, the overlap area of two circles is counted twice.

Let us study, by means of the two methods, the sets of 27 cosmic-ray events and of 422 AGN which maximize the Auger correlation. In the nearest-neighbour approach and for $\psi = 3.2^\circ$, we find $p \approx 0.21$, the number of correlated pairs is 20 at 5.6 expected by chance, so $P_{\rm min} \approx 5 \times 10^{-9}$ in agreement with the Auger claim. In the correlation-function approach, $p \approx 0.336$, the number of correlated pairs is 25 at 8.4 expected by chance, so $P_{\rm min} \approx 1.7 \times 10^{-3}$, several orders of magnitude higher[d]. In the case under discussion, these two differ qualitatively: when $P_{\rm min}$ is multiplied by the penalty factor $\sim 10^4$, the nearest-neighbour mehtod gives, as discussed above, a significant signal, while the correlation-function result is consistent with absence of any correlation.

This particularly strange pattern of correlation signals suggests that, if the signal is not a chance fluctuation, then the "nearest neighbours" of correlated events should be the actual sources of cosmic rays. In the rest of the paper, we will therefore study the properties of these "nearest neighbours".

[d]In the latter case, the binomial formula used in Refs. [3,4] is not applicable; $P_{\rm min}$ is estimated by the Monte-Carlo simulations.

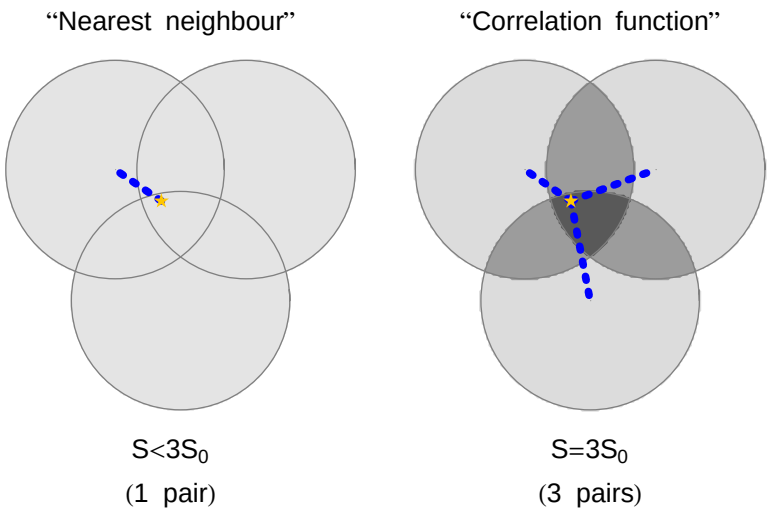

Fig. 1. Illustration of two approaches to estimate the correlation signal for clustered sources. Suppose that the circles of radius ψ (area S_0) around $k > 1$ potential sources (grey circles on the plot; $k = 3$ in this example) overlap and the cosmic-ray arrival direction (star) falls in the overlapping region. In the nearest-neighbour approach (left panel), each cosmic-ray event is associated with only one source; the area S covered by circles on the sky is counted once independently of overlaps. In the correlation-function approach (right panel), each pair "source–event" is counted ($k = 3$ pairs in the example) and the overlapping area is counted k times in the calculation of S.

3. Physical conditions in the correlated galaxies

The list of the sources responsible for the Auger correlation is given in Table 1. In this section, we analyze available data on physical conditions in these galaxies and compare them with requirements for UHECR acceleration discussed in Ref. [7].

3.1. *The central black holes*

We start with the analysis of conditions close to the central black holes of the correlated galaxies. Following the results of Ref. [7], we estimate the maximal possible energy of UHECR particles with atomic mass A and charge Z from the central black hole of mass $M_{\rm BH}$:

$$E_{\rm max} \simeq 3.7 \times 10^{19}\ {\rm eV} \frac{A}{Z^{1/4}} \left(\frac{M_{\rm BH}}{10^8 M_\odot} \right)^{3/8} . \qquad (1)$$

For a few objects, the mass of the black hole has been estimated previously in the literature; for others, we estimate $M_{\rm BH}$ from available data.

Methods of determination of the mass $M_{\rm BH}$ of the AGN central black hole have been reviewed in Ref. [32] (for a recent update, see e.g. [33]), where basic corresponding

references can be found. For 3 of 17 galaxies correlated with Auger events, $M_{\rm BH}$ has been estimated in the literature using observations of circumnuclear dynamics by means of:

(GD): resolved **gas dynamics**;

(MM): observations of accretion-disk **megamasers**;

(Hα): width of the **Hα line**.

For other galaxies in the sample we used, depending on the data availability, the following methods.

(SVD): **stellar velocity dispersion**. This quantity, σ, was found to be correlated with $M_{\rm BH}$; we use the relation [33]

$$\log\left(\frac{M_{\rm BH}}{10^8 M_\odot}\right) = (-0.08 \pm 0.02) + (3.93 \pm 0.10) \log\left(\frac{\sigma}{200\ {\rm km\,s^{-1}}}\right).$$

For some of the galaxies, σ is given in the LEDA database [34]; for a few others, we found it in the literature.

(KSB): **buldge K_s magnitude**. It is also correlated with $M_{\rm BH}$; we use the relation [35]

$$\log\left(\frac{M_{\rm BH}}{10^8 M_\odot}\right) = (-2.5 \pm 0.6) + (-0.45 \pm 0.03)\, K_s^0,$$

where the absolute bulge magnitude K_s^0 is related to the observed bulge magnitude K_s^B through

$$K_s^0 = K_s^B + A_K + {\rm DM}.$$

Here A_K is the correction for the Galactic extinction in the K band [36] and DM is the distance modulus (both A_K and DM are given in NED). For some of the galaxies, K_s^B was determined by the disk-bulge decomposition in previous studies; when known, it is often quoted in NED.

(KSM): **bulge K_s from morphology**. When K_s^B is not directly available, one may estimate it from the total K_s magnitude and the Hubble morphological type T of a galaxy by using the following relation [35],

$$K_s^B = K_s + 0.297\,(T+5) - 0.040\,(T+5)^2 + 0.0035\,(T+5)^3\,.$$

The precision of this relation is of order $0.5^{\rm m}$ and depends on T [35]. While this method is the least precise, it may be used to estimate $M_{\rm BH}$ for any galaxy with known distance because either K_s or a lower limit on it may be determined from the 2MASS full-sky survey data. For 9 of 17 correlated galaxies, KSM is the only available method to estimate $M_{\rm BH}$.

The data we use are collected in Table 2 while the summary of $M_{\rm BH}$ estimates is given in Table 3. For estimates of the maximal energy of cosmic-ray particles we always use the most precise estimate of the black-hole mass given in the bold face in Table 3. When different methods are applicable, less precise estimates are in a good agreement with better ones (a comparison plot is given in Fig. 2).

Figure 3 compares the maximal attainable energy $E_{\rm max}$ for protons and nuclei

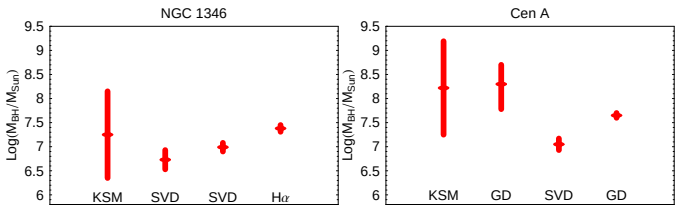

Fig. 2. Different estimates of the mass of the central black hole in two galaxies studied in Sec. 3. Letters denote the method of estimation (see Sec. 3.1).

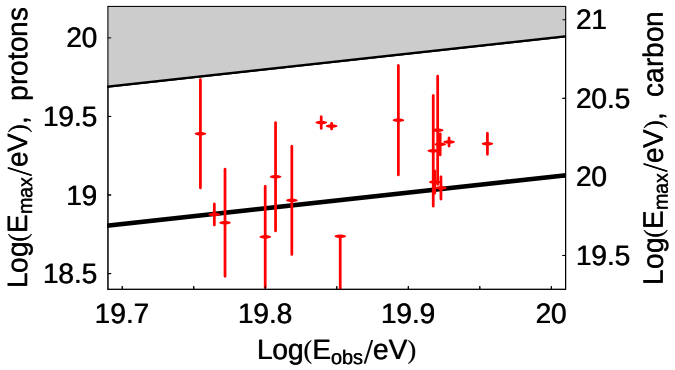

Fig. 3. The maximal energy $E_{\rm max}$ attainable by protons and carbon nuclei in the vicinity of the central black hole of individual active galaxies correlated with the Auger events, versus the energy $E_{\rm obs}$ of the observed cosmic-ray particle associated with the same galaxy (if a source corresponds to two events, $E_{\rm obs}$ is the highest one). The shaded area corresponds to the allowed region $E_{\rm obs} \leq E_{\rm max}$ for protons; the area above the thick black line corresponds to the allowed region $E_{\rm obs} \leq E_{\rm max}$ for carbon nuclei. The error bars correspond to precision of determination of the black-hole mass; Znajeck conservative upper limit for the magnetic field is assumed (see Ref. [7] for details). For PC 2207+0122, a dwarf galaxy associated with two cosmic-ray events but not detected in the 2MASS survey, only an upper limit on $E_{\rm max}$ is available.

near the central black hole of the galaxies with actual energies of the correlated cosmic-ray events. The energy $E_{\rm max}$ has been calculated using Eq. (1). We remind that this equation gives an upper limit on $E_{\rm max}$ which is lower in particular models and for realistic values of the magnetic fields. Central black holes of any of these galaxies cannot accelerate protons to the observed energies. While they could be able to accelerate heavier nuclei, deflections of these nuclei in the Galactic magnetic field would spoil the directional correlation at $\psi \sim 3^\circ$.

3.2. *Jets and other extended structures*

In eight of the correlated galaxies, extended nuclear outflows have been detected. Except for Cen A, which is discussed separately in the following section, these

outflows are most probably non-relativistic, and when the origin of the emission may be determined, it is thermal. Observations of outflows in correlated Seyfert galaxies are summarized in Table 4. Magnetic fields in these outflows have not been studied; to get order-of-magnitude estimates, we assume that the energy of the magnetic field is the same as the total energy of the radiation field. We assume a spherical source of the radius $R/2$ filled with magnetic field B, so that the energy of the magnetic field is $E_1 \sim \pi R^3 B^2/6$. The energy of the radiation field may be estimated as $E_2 \sim R\,dE_2/dt$, where the energy loss $dE_2/dt = 4\pi D^2 \int I_\nu\, d\nu$ for a source at the distance D with the observed flux I_ν at the frequency ν (we use the definition of I_ν as the energy per unit area per unit time per unit frequency interval per unit solid angle, that is I_ν is measured e.g. in Jansky). Within our precision, $\int I_\nu\, d\nu \sim I_\nu \nu$. Equating $E_1 = E_2$ and expressing D/R through the angular size of the source θ, we arrive at

$$B \sim 6.5 \times 10^{-6}\ \mathrm{G}\ \left(\frac{\theta}{\mathrm{mas}}\right)^{-1} \left(\frac{I}{\mathrm{mJy}}\right)^{1/2} \left(\frac{\nu}{\mathrm{GHz}}\right)^{1/2}. \qquad (2)$$

Estimated magnetic fields (given in Table 4) do not exceed those expected for normal galaxies of the same size; the outflows certainly cannot serve as acceleration sites of UHECRs because they do not satisfy the Hillas criterion.

3.3. *The case of* Centaurus A

One of the correlated galaxies, NGC 5128, hosts a radio galaxy known as Cen A. Due to its proximity, it represents a textbook example of FR I radio galaxy, studied in great details for decades. It has been suggested long ago as a source of some [49,50] or even most [51,52] of the observed cosmic rays of extreme energies. Both the original [3] and some of the alternative [11,12,13,14,19,23] interpretations of the Auger correlation signal imply that Cen A is a UHECR source. We therefore devote a separate section to the study of physical conditions in Cen A.

Centaurus A (for reviews, see Refs. [53,54] and a continuously updated webpage [55]) is a low-power radio galaxy (its luminosity is intermediate between Seyfert and FR I [56]) which, most probably, experienced a major merging event recently. High-resolution studies determine the compact nucleus (optically classified as Seyfert 2) whose multifrequency spectral energy distribution is very similar to those of the BL Lac type objects (see Refs. [56,57,58,59] for discussion[e]); the jet which experience several bendings observed at scales from light months [60] to dozens of kiloparsecs from the nuclei; inner radio lobes associated with the jet and giant outer radio lobes which span about 9° on the sky. The jet is mildly relativistic, $\Gamma < 2.5$ at parsec scales [56] (velocity $\sim 0.45c$ was inferred [61] and proper motions $\sim 0.12c$ were observed [62]). Polarization studies reveal that the magnetic field in

[e]Cen A is the only object in the AGN sample studied by PAO which is classified as a BL Lac in the Véron catalog [6].

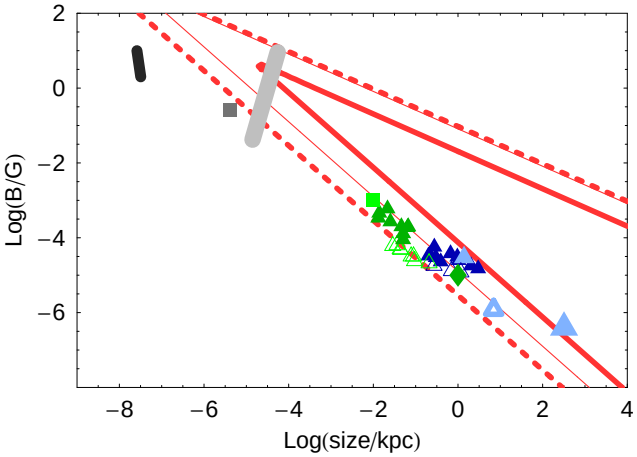

Fig. 4. The size-field plot for different parts of Cen A. Grey colours: the nuclear region (light-grey error-bar diagonal, radio-to-X-ray modelling of Ref. [68]; dark-grey error-bar diagonal, that of Ref. [69]; grey box, synchrotron self-absorption measurement of Ref. [56]). Green colours: the jet (small green triangles, minimal-pressure estimates for resolved components [70]; light-green empty triangles, equipartition estimates for resolved components [71]; green box, model estimate for a knot [72]; green diamond, model estimate for the possible hard-spectrum shear layer [66]). Blue colours: the lobes (large light-blue triangle, equipartition estimate for the giant outer lobes [73] (see also Ref. [74]); other points are estimates for inner lobes: small light-blue triangle, minimal-energy [75]; small empty light-blue triangle, equipartition [73]; dark-blue triangles, minimal-pressure [70]; dark-blue empty triangles, equipartition [71]). The allowed region for acceleration of 7×10^{19} eV particles is located between red lines (thick, protons; thin, carbon nuclei; dashed, iron nuclei; lower lines corresponds to the Hillas limit, upper ones corresponds to the radiation-loss limit for diffusive acceleration). Note that the diffusive-acceleration loss limit is determined by A/Z and is therefore indistinguishable for iron ($A = 56$, $Z = 26$) and carbon ($A = 12$, $Z = 6$). See Ref. [7] for details of the calculation of allowed areas and for description of the methods to estimate the magnetic fields.

the jet is parallel to the jet axis at the scales of at least 3 kpc (see e.g. Ref. [63] and references therein). Several dosen knots are resolved in the jet; their radio and X-ray positions are systematically offset from each other (see e.g. Ref. [64]). These knots are possible sites of particle acceleration; however recent X-ray observations (e.g. [65]) suggest that another, distributed along the jet, acceleration mechanism should be at work. This mechanism may be associated with a hard-spectrum shear layer possibly observed along the kiloparsec-scale jet [66]. Multifrequency observations (e.g. Ref. [67]) establish the synchrotron origin of the jet emission with high confidence.

Numerous estimates of the magnetic field in different parts of Cen A are summarized in Fig. 4. Acceleration of protons to the energy of 7×10^{19} eV (the energy of the events associated with the Cen A nucleus by PAO) is hardly possible in this source, except maybe for the giant outer lobes which are however displaced from the nucleus by an angular distance exceeding $\psi = 3.2°$. On the other hand, acceler-

ation of intermediate-mass and heavy nuclei in the jet and lobes of Cen A remains a plausible interpretation of the correlation signal.

4. Conclusions

The correlations observed by PAO may be explained either by the AGN hypothesis or by chance coincidence. The AGN hypothesis implies that the primary cosmic-ray particles are protons and has three options:

(i) the correlated AGN are (some of) the sources;

(ii) the AGN as a whole are sources; particular correlated AGN may not be the actual sources if they are located in regions of enhanced AGN density;

(iii) the sources are not AGN but follow a similar distribution in space, that is, like AGN, they follow the local large-scale structure of the Universe.

The options (iii) and (ii) are disfavoured by the absence of the events from the direction of the Virgo supercluster [11]; the options (i) and (ii) are disfavoured by the luminosity argument [18].

In this paper we have noted that (ii) and (iii) are also disfavoured by the disappearence of correlations in terms of the correlation-function approach, contrary to the nearest-neighbour probability estimate. In order to test the option (i), we have studied physical conditions in particular correlated galaxies. Most of them are low-power Seyfert galaxies; we have demonstrated that **none of the correlated AGN can accelerate protons to the observed energies**, thus excluding the option (i) and giving further support to the explanation of correlations by means different than the AGN hypothesis.

Our results suggest that the correlated galaxies, notably Cen A, can accelerate nuclei to the observed energies. The deflections would however spoil the small-angle correlations, but the origin of a significant part of the detected particles in Cen A jet and lobes remains one of the most probable explanations for the observed anisotropy.

Note added

Recently, a few months after this paper was completed and posted in arXiv, PAO released (see e.g. Ref. [76]) information about tests of the AGN correlations with new data. In agreement with our results, these data speak against the AGN interpretation of the observed anisotropy: among 31 events with $E > E_{\rm min}$ recorded after publication of Ref. [3] and before March 2009, 8 correlate with AGN while 6.5 chance coincidences are expected for isotropic distribution of arrival directions [76].

Acknowledgments

The authors are indebted to D. Gorbunov, G. Rubtsov, L. Stawarz, P. Tinyakov and I. Tkachev for discussions. We acknowledge the use of online tools [31,34,55]. This work was supported in part by the grants RFBR 07-02-00820, RFBR 09-07-00388, NS-1616.2008.2 (ST), by FASI under state contracts 02.740.11.0244 (ST) and 02.740.11.5092 (SG and ST) and by the Dynasty Foundation (ST).

References

1. D. F. Torres and L. A. Anchordoqui, Rept. Prog. Phys. **67**, 1663 (2004) [arXiv:astro-ph/0402371].
2. D. S. Gorbunov and S. V. Troitsky, Astropart. Phys. **23**, 175 (2005) [arXiv:astro-ph/0410741].
3. J. Abraham *et al.* [Pierre Auger Collaboration], Science **318**, 938 (2007) [arXiv:0711.2256 [astro-ph]].
4. J. Abraham *et al.* [Pierre Auger Collaboration], Astropart. Phys. **29**, 188 (2008) [Erratum-ibid. **30**, 45 (2008)] [arXiv:0712.2843 [astro-ph]].
5. P.L. Biermann and P. A. Strittmatter, Astrophys. J. **322**, 643 (1987)
6. M.P. Véron-Cetty and P. Véron, Astron. Astrophys. **455** 773 (2006)
7. R. Ptitsyna and S. Troitsky , arXiv:0808.0481[astro-ph]
8. P. Tinyakov and I. Tkachev, Phys. Rev. D **69**, 128301 (2004) [arXiv:astro-ph/0301336].
9. C. B. Finley and S. Westerhoff, Astropart. Phys. **21**, 359 (2004) [arXiv:astro-ph/0309159].
10. D. Harari [The Pierre Auger Collaboration], arXiv:0706.1715 [astro-ph].
11. D. Gorbunov, P. Tinyakov, I. Tkachev and S. V. Troitsky, JETP Lett. **87**, 461 (2008) [arXiv:0711.4060 [astro-ph]].
12. D. Fargion, Phys. Scripta **78**, 045901 (2008) [arXiv:0801.0227 [astro-ph]].
13. T. Wibig and A. W. Wolfendale, arXiv:0712.3403 [astro-ph].
14. D. S. Gorbunov, P. G. Tinyakov, I. I. Tkachev and S. V. Troitsky, arXiv:0804.1088 [astro-ph].
15. M. Unger [The Pierre Auger Collaboration], arXiv:0706.1495 [astro-ph].
16. A. V. Glushkov *et al.*, JETP Lett. **87**, 190 (2008) [arXiv:0710.5508 [astro-ph]]
17. K. Kotera and M. Lemoine, Phys. Rev. D **77**, 123003 (2008) [arXiv:0801.1450 [astro-ph]].
18. L.G. Dedenko *et al.*, arXiv:0804.4582 [astro-ph].
19. I. V. Moskalenko, L. Stawarz, T. A. Porter and C. C. Cheung, Astrophys. J. **693**, 1261 (2009) [arXiv:0805.1260 [astro-ph]].
20. M. R. George *et al.*, arXiv:0805.2053 [astro-ph].
21. T. Stanev, arXiv:0805.1746 [astro-ph].
22. G. Ghisellini *et al.*, arXiv:0806.2393 [astro-ph]
23. N. M. Nagar and J. Matulich, arXiv:0806.3220 [astro-ph].
24. R. U. Abbasi *et al.* [HiRes Collaboration], Astropart. Phys. **30**, 175 (2008) [arXiv:0804.0382 [astro-ph]].
25. A. A. Ivanov, Pisma Zh. Eksp. Teor. Fiz. **87**, 215 (2008) [JETP Lett. **87**, 185 (2008)] [arXiv:0803.0612 [astro-ph]].
26. V. A. Lipovetsky, S. I. Neizvestny and O. M. Neizvestnaya, *Comm. SAO* **55** 5 (1988)
27. A. V. Uryson, J. Exp. Theor. Phys. **89** 597 (1999)
28. A. V. Uryson, arXiv:astro-ph/0303347.
29. P. G. Tinyakov and I. I. Tkachev, JETP Lett. **74**, 445 (2001) [Pisma Zh. Eksp. Teor. Fiz. **74**, 499 (2001)] [arXiv:astro-ph/0102476].
30. D. S. Gorbunov, P. G. Tinyakov, I. I. Tkachev and S. V. Troitsky, JETP Lett. **80**, 145 (2004) [Pisma Zh. Eksp. Teor. Fiz. **80**, 167 (2004)] [arXiv:astro-ph/0406654].
31. The NASA/IPAC Extragalactic database (available at http://nedwww.ipac.caltech.edu).
32. F. Ferrarese and H. Ford, Space Science Reviews **116** 523 (2005)
33. J. Shen *et al.*, Astron. J. **135** 928 (2008) [arXiv:0712.1630 [astro-ph]]
34. G. Paturel *et al.*, Astron. Astrophys. **412** 45 (2003); http://leda.univ-lyon1.fr
35. X. Dong and M. M. De Robertis, Astron. J. **131**, 1236 (2006)

[arXiv:astro-ph/0510694].
36. D. J. Schlegel, D. P. Finkbeiner and M. Davis, Astrophys. J. **500**, 525 (1998) [arXiv:astro-ph/9710327]; http://astro.berkeley.edu/dust/index.html
37. Z. X. Peng, Q. S. Gu, J. Melnick and Y. H. Zhao, Astron. Astrophys. **453** 863 (2006) [arXiv:astro-ph/0603849]
38. L. J. Greenhill, J. M. Moran and J. R. Herrnstein, Astrophys. J. **481** L23 (1997)
39. R. C. Y. Chou *et al.*, Astrophys. J. **670** 116 (2007) [arXiv:0709.3960 [astro-ph]]
40. N. Neumayer *et al.*, Astrophys. J. **671** 1329 (2007) [arXiv:0709.1877 [astro-ph]]
41. A. Marconi *et al.*, Astrophys. J. **549** 915 (2001)
42. E. J. M. Colbert *et al.*, Astrophys. J. **496** 786 (1998) [arXiv:astro-ph/9711137]
43. A. L. Kinney *et al.*, Astrophys. J. **537** 152 (2000)
44. N. M. Nagar *et al.*, Astrophys. J. Suppl. **120** 209 (1999) [arXiv:astro-ph/9901236]
45. J. I. Harnett *et al.*, Astron. Astrophys. **216** 39 (1989)
46. N. J. Schurch, T. P. Roberts and R. S. Warwick, Mon. Not. Roy. Astron. Soc. **335**, 241 (2002) [arXiv:astro-ph/0204361].
47. A. Thean *et al.*, Mon. Not. Roy. Astron. Soc. **314** 573 (2000), [arXiv:astro-ph/0001459]
48. E. Middelberg *et al.*, Astron. Astrophys. **417**, 925 (2004) [arXiv:astro-ph/0402142].
49. G. Cavallo, *Astron. Astrophys.* **65** 415 (1978)
50. G. E. Romero, J. A. Combi, L. A. Anchordoqui and S. E. Perez Bergliaffa, Astropart. Phys. **5**, 279 (1996) [arXiv:gr-qc/9511031].
51. G. R. Farrar and T. Piran, arXiv:astro-ph/0010370.
52. L. A. Anchordoqui, H. Goldberg and T. J. Weiler, Phys. Rev. Lett. **87**, 081101 (2001) [arXiv:astro-ph/0103043].
53. F. P. Israel, Astron. Astrophys. Rev. **8** 237 (1998)
54. H. Steinle, Chin. J. Astron. Astrophys. **6** 106 (2006)
55. H. Steinle, http://www.mpe.mpg.de/Cen-A
56. K. Meisenheimer *et al.*, Astron. Astrophys. **471** 453 (2007) [arXiv:0707.0177 [astro-ph]]
57. R. Morganti *et al.*, Mon. Not. Roy. Astron. Soc. **256** 1 (1992)
58. M. Chiaberge, A. Capetti and A. Celotti, Mon. Not. Roy. Astron. Soc. **324**, L33 (2001) [arXiv:astro-ph/0105159].
59. J. M. Bai and M. G. Lee, Astrophys. J. **549**, L173 (2001) [arXiv:astro-ph/0102314].
60. PASJ-52-1021 K. Fujisawa *et al.*, Pub. Astron. Soc. Japan **52** 1021 (2000)
61. S. J. Tingay *et al.*, Astron. J. **115** 960 (1998)
62. S.J. Tingay, R. A. Preston and D. L. Jauncey, Astron. J. **115** 960 (2001)
63. M. J. Hardcastle *et al.*, Astrophys. J. **593** 169 (2003)
64. R. P. Kraft *et al.*, Astrophys. J. **569** 54 (2002)
65. M. J. Hardcastle *et al.*, Astrophys. J. **670** L81 (2007) [arXiv:0710.1277 [astro-ph]]
66. J. Kataoka *et al.*, Astrophys. J. **641** 158 (2006) [arXiv:astro-ph/0510661]
67. M. J. Hardcastle, R. P. Kraft and D. M. Worrall, Mon. Not. Roy. Astron. Soc. Lett. **368**, L15 (2006) [arXiv:astro-ph/0601421].
68. J. H. Beall and W. K. Rose, *Astrophys. J.* **238** 539 (1980)
69. J. P. Lenain *et al.*, Astron. Astrophys. **478** 111 (2008) [arXiv:0710.2847 [astro-ph]]
70. D. A. Clarke, J. O. Burns and M. L. Norman, Astrophys. J. **395** 444 (1992)
71. J. O. Burns, E. D. Feigelson and E. J. Schreier, Astrophys. J. **273** 128 (1983)
72. J. Mao and J. Wang, Astrophys. J. **669** L13 (2007) [arXiv:0709.2210 [astro-ph]]
73. H. Alvarez *et al.*, Astron. Astrophys. **355** 863 (2000)
74. M. J. Hardcastle, C. C. Cheung, I. J. Feain and L. Stawarz, Mon. Not. Roy. Astron. Soc. **393** 1041 (2009) [arXiv:0808.1593 [astro-ph]]
75. M. H. Brookes *et al.*, Astrophys. J. **646** L41 (2006)

76. D. Martello et al. [Pierre Auger Collaboration], Talk at Scineghe 2009, Assisi, Italy; available from `http://agenda.infn.it/materialDisplay.py?contribId=27&amp;sessionId=8&amp;materialId=slides&amp;confId=1369`

Table 1. Active galaxies correlated with Auger events. Col. (1) gives the source name, Col. (2) gives the energy(ies) of the cosmic-ray particles for which this source is the "nearest neighbour" in the correlated sample; Col. (3) gives the distance to the object (taken from NED [31]); in Cols. (4) to (6) objects detected in radio (R), X rays (X) and gamma rays with $E > 1$ MeV (γ) are marked with +; Col. (7) gives the AGN type (mostly from NED: Seyfert galaxies (Sy), galaxies with H II regions (HII), emission-line dwarf galaxy (EmG) and FR I radio galaxy (FRI)); Col. (8) gives the estimated mass of the central black hole (see Sec. 3.1 and Table 3 for details and error bars). Objects with relativistic jets (J) and non-relativistic outflows (O) are marked in Col. (9), and the object with knots (K), hot spots (H) and lobes (L) is marked in Col. (10).

Object	E	d	detection			AGN	$\log\left(\frac{M_{\rm BH}}{M_\odot}\right)$	jets	knots,
	(EeV)	(Mpc)	R	X	γ	type			lobes
(1)	(2)	(3)	(4)	(5)	(6)	(7)	(8)	(9)	(10)
ESO 383-G18	84	51	+	+	−	Sy2	6.60	O	–
4U 1344-60	66	51	−	+	−	Sy1.5	6.39	–	–
ESO 139-G12	83, 59	68	−	−	−	Sy2	7.23	–	–
IC 4518A	63	66	+	+	−	Sy2	5.77	–	–
NGC 424	84	46	+	+	−	Sy2	7.34	O	–
NGC 4945	58	5	+	+	−	Sy2	6.15	O	–
IC 5169	57	42	+	−	−	Sy2	7.52	O	–
CGCG 374-029	59	58	+	−	−	Sy1	6.01	–	–
NGC 1346	85	54	+	−	−	Sy1	7.38	–	–
NGC 7591	83	69	+	−	−	Sy	7.58	–	–
NGC 1358	69	54	+	+	−	Sy2	7.71	O	–
Cen A	69, 70	5	+	+	+	FRI	7.65	J	K,H,L
PC 2207+0122	58, 71	55	−	−	−	EmG	<5.76	–	–
NGC 2989	64	56	+	−	−	HII	6.79	–	–
NGC 1204	78	57	+	−	−	HII	7.75	–	–
NGC 7130	90	65	+	+	−	Sy2	7.35	O	–
NGC 5506	83	29	+	+	−	Sy2	6.70	O	–

Table 2. Data used to estimate the mass of the central black hole in active galaxies correlated with Auger events. Col. (1): the source name. Col. (2): K_s magnitude (A: 95% confidence-level lower limit from the 2MASS point source rejection table; B: bulge decomposed magnitude from Ref. [37], C: buldge decomposed magnitude from Ref. [35], D: DENIS value from LEDA, no letter: 2MASS value from NED; for B and C, 2MASS error bars assumed). Col. (3): correction for Galactic extinction in K band (Ref. [36], NED). Col. (4): distance modulus (NED; accuracy is $\pm 0.15^{\mathrm{m}}$ except for PC 2207+0122 ($\pm 0.21^{\mathrm{m}}$). Col. (5): Hubble morphological type from LEDA. Col. (6): central velocity dispersion (star denotes data from Ref. [37] for which 10% accuracy was assumed in calculations, if no reference given, data from LEDA).

Object (1)	K_s, mag (2)	A_K, mag (3)	DM, mag (4)	T (5)	σ, km/s (6)
ESO 383-G18	11.99 ± 0.05 B	0.022	33.52	0	92.3 *
4U 1344-60	11.140 ± 0.043	1.082	33.49	5	–
ESO 139-G12	9.709 ± 0.039	0.027	34.17	4	–
IC 4518A	11.09 ± 0.22 D	0.058	34.10	6	–
NGC 424	11.23 ± 0.02 B	0.006	33.31	0	142.6 *
NGC 4945	4.483 ± 0.017	0.065	28.43	4	127.9 ± 19.1
IC 5169	9.776 ± 0.029	0.006	33.10	0	–
CGCG 374-029	11.260 ± 0.050	0.043	33.80	5	–
NGC 1346	9.790 ± 0.029	0.019	33.66	3	116.1 ± 4.7 [33]
NGC 7591	9.602 ± 0.032	0.038	34.19	3	–
NGC 1358	10.18 ± 0.003 C	0.023	33.65	0	176.7 ± 10.1
Cen A	3.942 ± 0.016	0.042	28.39	-2	119.8 ± 7.1
PC 2207+0122	> 17.057 A	0.013	33.69	?	–
NGC 2989	10.229 ± 0.049	0.023	33.72	4	–
NGC 1204	9.947 ± 0.030	0.027	33.77	0	–
NGC 7130	10.18 ± 0.01 B	0.011	34.08	1	143.2 *
NGC 5506	10.74 ± 0.015 B	0.022	32.29	1	97.9 *

Table 3. The estimates of the mass of the central black hole of active galaxies correlated with Auger events. Col. (1) gives the source name, Col. (2) gives the mass estimate, Col. (3) gives the method (see Sec. 3.1), Col. 4 gives the reference to either the mass value (v) or the data used to calculate it (d). If no reference is given, the LEDA value of σ was used in the SVD method, and the data of Table 2 were used in the KSB, KSM method. The most precise estimates for each object, which we use in this work, are given in the bold face.

Object	$\log\left(\frac{M_{\rm BH}}{10^8 M_\odot}\right)$	Method	Reference
(1)	(2)	(3)	(4)
ESO 383-G18	$\mathbf{-1.40 \pm 0.19}$	SVD	[37] d
	-0.80 ± 0.88	KSB	
4U 1344-60	$\mathbf{-1.61 \pm 0.92}$	KSM	
ESO 139-G12	$\mathbf{-0.77 \pm 0.94}$	KSM	
IC 4518A	$\mathbf{-2.23 \pm 0.86}$	KSM	
NGC 424	$\mathbf{-0.66 \pm 0.18}$	SVD	[37] d
	-0.56 ± 0.90	KSB	
NGC 4945	$\mathbf{-1.85 \pm 0.18}$	MM	[38] v
	-0.98 ± 0.93	KSM	
	-0.84 ± 0.26	SVD	
	< -2	GD	[39] v
IC 5169	$\mathbf{-0.48 \pm 0.92}$	KSM	
CGCG 374-029	$\mathbf{-1.99 \pm 0.91}$	KSM	
NGC 1346	$\mathbf{-0.62 \pm 0.07}$	Hα	[33] v
	-0.75 ± 0.90	KSM	
	-1.27 ± 0.20	SVD	
	-1.01 ± 0.09	SVD	[33] d
NGC 7591	$\mathbf{-0.42 \pm 0.92}$	KSM	
NGC 1358	$\mathbf{-0.29 \pm 0.10}$	SVD	
	0.14 ± 0.95	KSM	
	0.07 ± 0.93	KSB	[35] d
Cen A	$\mathbf{-0.35 \pm 0.05}$	GD	[40] v
	0.22 ± 0.97	KSM	
	-0.95 ± 0.12	SVD	
	$0.30^{+0.40}_{-0.52}$	GD	[41] v
PC 2207+0122	$\mathbf{< -2.22}$	KSM	
NGC 2989	$\mathbf{-1.21 \pm 0.92}$	KSM	
NGC 1204	$\mathbf{-0.25 \pm 0.93}$	KSM	
NGC 7130	$\mathbf{-0.65 \pm 0.18}$	SVD	[37] d
	0.26 ± 0.93	KSB	
NGC 5506	$\mathbf{-1.30 \pm 0.19}$	SVD	[37] d
	-0.79 ± 0.89	KSB	
	-0.25 ± 0.20	SVD	

Table 4. Observations of outflows detected in correlated galaxies. Col. (1): the source name. Col. (2): linear size. Col. (3): frequency of observations. Col. (4): observed flux. Col. (5): estimate of the magnetic field (for kpc wind in NGC 5506, from thermal source model of Ref. [42]; for other cases, from Eq. (2)). Col. (6): reference to the data.

Object (1)	R, kpc (2)	ν, GHz (3)	F, mJy (4)	$B_{\rm est}$, G (5)	Ref. (6)
ESO 383-G18	0.107	8.3	1.7	2×10^{-7}	43
NGC 424	0.33	8.3	13.1	10^{-7}	43
	0.5	1.5	23.9	5×10^{-8}	44
		8.4	13.1	9×10^{-8}	44
NGC 4945	31.4	4.8	51	9×10^{-10}	45
	0.5	1.5×10^{18}	2.6×10^{-6}	10^{-7}	46
IC 5169	0.35	1.5	17.6	5×10^{-8}	44
		8.4	3.7	6×10^{-8}	44
NGC 1358	0.36	1.5	3.4	3×10^{-8}	44
		8.4	0.9	3×10^{-8}	44
Cen A			see Sec. 3.3		
NGC 7130	0.188	8.4	18.1	4×10^{-7}	47
NGC 5506	0.0015	8.4	24.4	3×10^{-5}	48
	0.36	8.4	67.6	10^{-7}	47
	$1.2\div3.0$	1.5×10^{18}	$(0.6\div2.4)\times10^{-7}$	$(0.8\div6)\times10^{-6}$	42
	0.302	8.3	95.0	2×10^{-7}	43

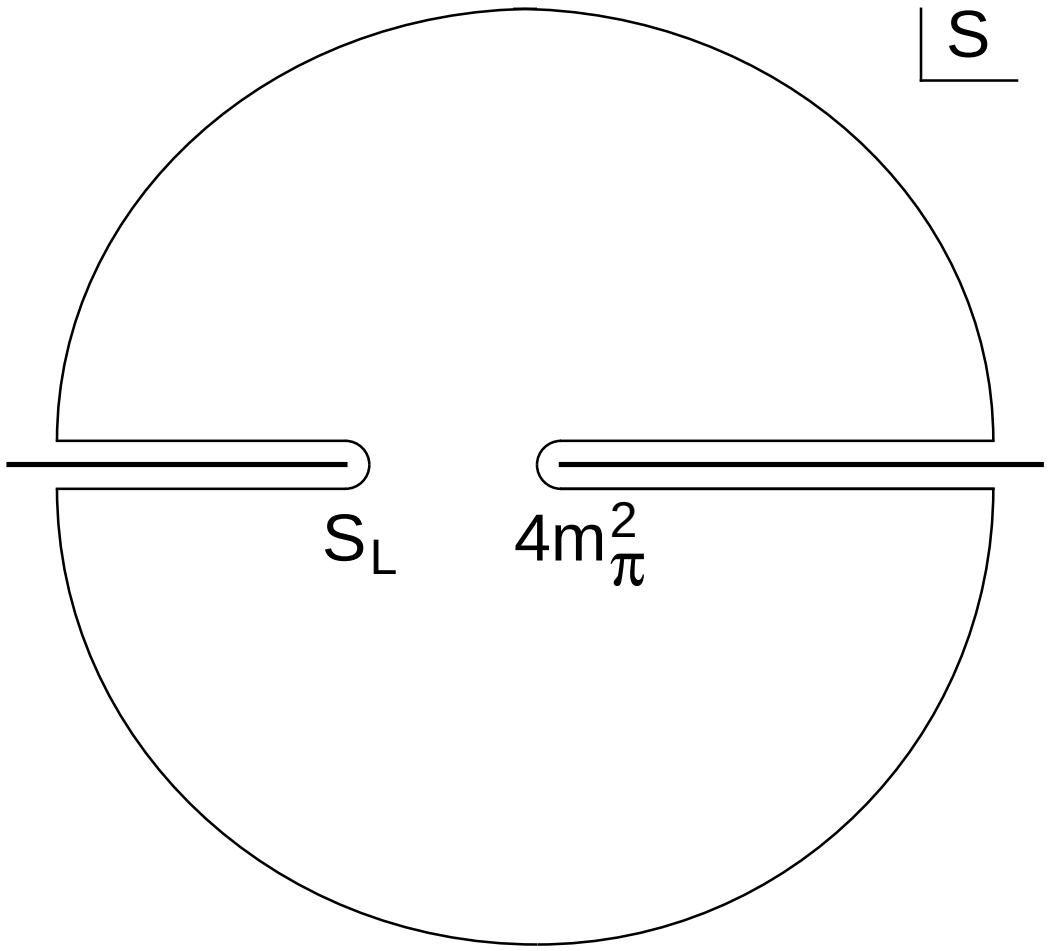
S
S_L
$4m_\pi^2$